

CONSTRUCTION AND ANALYSIS OF A NEW QUATERNIONIC SPACE-TIME CODE FOR 4 TRANSMIT ANTENNAS*

ROBERT CALDERBANK[†], SUSHANTA DAS[‡], N. AL-DHAHIR[‡], AND S. DIGGAVI[§]

Dedication

We dedicate this paper to Professor Thomas Kailath on the occasion of his 70th birthday. We have been greatly influenced by his way of attacking engineering problems by exploiting their inherent mathematical structure. This paper is an example of this research paradigm, where nineteenth century mathematics is used to significantly improve the performance of 21st century wireless infrastructure.

Abstract. We present a novel full-rate full-diversity orthogonal space-time block code for QPSK modulation and 4 transmit antennas based on quaternionic algebra. The code does not result in constellation expansion unlike other full-rate full-diversity codes in the literature. The quaternionic structure of the code is exploited to reduce the complexity of maximum likelihood (ML) coherent decoding from a size-256 search to a size-16 search. Furthermore, we show how to modify this low-complexity coherent ML decoding rule to derive a non-coherent differential ML decoding rule. Due to the orthogonality of the code, ML differential decoding results in the minimum SNR loss of 3 dB from coherent ML decoding. Finally, extensive simulation results in a WiMAX 802.16 broadband wireless access environment demonstrate that the proposed code increases the cell coverage area by 1.5 and 2.6 folds compared to single-antenna transmission at 10^{-3} bit error rate when combined with 1 and 2 receive antenna(s), respectively.

1. Introduction. WiMAX is an emerging wireless technology that promises to deliver broadband connectivity with a data rate up to 75 Mbps over a 20 MHz bandwidth and a coverage radius up to 6 miles. To achieve such a range and high data rate, the IEEE 802.16-2004 standard supports multiple-antenna techniques including space-time coding (STC). The information-theoretic analyses in [1, 2] showed that multiple antennas at the transmitter and receiver enable very high-data-rate reliable wireless communications. STC introduced in [3], improve the reliability of communication over fading channels by correlation of signals across the different transmit antennas. A characterization of the design criteria of such codes was given in [3, 4]. One class of STC are space-time block codes (STBC) introduced in [6, 5] which are the technical focus of this paper.

Orthogonal designs [5] are a class of STBC that achieve maximal diversity at a linear (in constellation size) decoding complexity. However, the only full-rate complex

*This work was presented in part at the IEEE ISIT'04 and IEEE VTC Fall'05 conferences. The work of N. Al-Dhahir is supported in part by the Texas Advanced Technology (ATP) program project no.009741-0023-2003 and by NSF project no. 0430654

[†]Princeton University, New Jersey, USA. E-mail: calderbank@math.princeton.edu

[‡]University of Texas at Dallas, Texas, USA. E-mail: {sushanta,aldhahir}@utdallas.edu

[§]EPFL, Laussane, Switzerland. E-mail: suhas.diggavi@epfl.ch

orthogonal design is the 2×2 Alamouti code [6], and as the number of transmit antennas increases, the available rate becomes unattractive. For example, for 4 transmit antennas (which is the case of interest in this paper), orthogonal STBC designs with rates of $\frac{1}{2}$ and $\frac{3}{4}$ were presented in [5]. This rate limitation of orthogonal designs caused a recent shift of research focus to non-orthogonal code design. These include a quasi-orthogonal design for 4 transmit antennas [13] that has rate 1 but achieves only diversity of two (for one receive antenna). Full diversity can be achieved by including signal rotations which expand the constellation (see e.g. [15]). Another approach is the design of non-orthogonal but linear codes [7, 8, 9, 11], for which decoding [10] is efficient (using the sphere decoding algorithm [21]) though the decoding complexity depends on the channel realization. Some of these constructions also involve rotation of signal constellations and result in significant constellation expansion. In this paper, we revisit the problem of designing orthogonal STBC for 4 transmit antennas. Another reason for our interest in orthogonal designs is that they limit the SNR loss incurred by differential decoding to its minimum of 3 dB from coherent decoding.

The main contribution of this paper is the design and analysis of a novel full-rate full-diversity orthogonal STBC for 4 transmit antennas. This code is constructed by means of a 2×2 array over the quaternions, thus resulting in a 4×4 array over the complex field \mathbf{C} . The code is orthogonal over \mathbf{C} , but is *not* linear. The structure of the code is a generalization of the 2×2 Alamouti code [6], and reduces to it if the 2×2 quaternions in the code are replaced by complex numbers. For QPSK modulation, the code has no constellation expansion and enjoys a simple maximum likelihood decoding algorithm. We also develop a differential encoding and decoding algorithm for this code.

After presenting this work at the DIMACS workshop [18], we became aware of the work in [19] in which the authors independently present the same code and show by simulation that it achieves full diversity and no constellation expansion for QPSK. This work is distinct from [19] in the following aspects. We establish rigorously the connection of our code design to the theory of quaternions. This enables us to prove analytically the full-diversity result for a general M -PSK constellation (not only for QPSK). Moreover, the connection to quaternions leads to new examples, to an efficient ML decoding algorithm for 1 receive antenna, and to extensions to multiple receive antennas. We also develop a differential version of the code and investigate its performance for the WiMAX application.

This paper is organized as follows. In Section 2, we start with the data model and some background on quaternions. In Section 3, we introduce the 4×4 STBC and prove that it achieves maximum diversity order. In Section 4, we develop a low-complexity coherent decoding algorithm that utilizes the quaternionic structure of the non-linear orthogonal STBC. Section 5 develops a differential encoding and decoding algorithm for the code. Simulation results are presented in Section 6 and the paper

is concluded in Section 7.

2. Preliminaries.

2.1. Data Model. Our focus in this paper is on the quasi-static flat-fading channel where we transmit information coded over $M_t = 4$ transmit antennas and employ M_r antennas at the receiver. We assume that the transmitter has no channel state information (CSI), whereas the receiver is able to perfectly track the channel (a common assumption, see [3]).¹ The code is designed over a coherence time of $T = M_t = 4$ transmission symbols and the received signal after demodulation and sampling can be written as

$$(1) \quad \mathbf{R} = \mathbf{H}\mathbf{X} + \mathbf{Z},$$

where $\mathbf{R} = [\mathbf{r}(0), \dots, \mathbf{r}(T-1)] \in \mathbf{C}^{M_r \times T}$ is the received signal matrix, $\mathbf{H} \in \mathbf{C}^{M_r \times M_t}$ is the quasi-static channel matrix, $\mathbf{X} = [\mathbf{x}(0), \dots, \mathbf{x}(T-1)] \in \mathbf{C}^{M_t \times T}$ is the space-time-coded transmitted signal matrix with transmit power constraint P , and $\mathbf{Z} = [\mathbf{z}(0), \dots, \mathbf{z}(T-1)] \in \mathbf{C}^{M_r \times T}$ is additive white Gaussian noise with variance σ^2 .

The coding scheme is limited to one quasi-static transmission block. Similar arguments can be made if we are allowed to code across only a *finite* number of quasi-static transmission blocks [3]. This allows us to view the channel in (1) as a non-ergodic channel since the performance is determined by a single randomly-chosen channel fading matrix \mathbf{H} . In this context we define the notion of diversity order [3] as follows.

DEFINITION 2.1. *A coding scheme with an average error probability $\bar{P}_e(\text{SNR})$ as a function of SNR that behaves as*

$$(2) \quad \lim_{\text{SNR} \rightarrow \infty} \frac{\log(\bar{P}_e(\text{SNR}))}{\log(\text{SNR})} = -d$$

is said to have a diversity order of d .

In words, a scheme with diversity order d has an error probability at high SNR behaving as $\bar{P}_e(\text{SNR}) \approx \text{SNR}^{-d}$.

2.2. Code Design Criteria. For codes designed for a finite (and fixed) rate, one can bound the error probability by using *pairwise error probability* (PEP) between two candidate codewords. This leads to the rank criterion for determining the diversity order of a space-time code [3, 4]. Consider a codeword sequence $\mathbf{X} = [\mathbf{x}^T(0), \dots, \mathbf{x}^T(T-1)]$ as defined in (1), where $\mathbf{x}(k) = [\mathbf{x}_1(k), \dots, \mathbf{x}_{M_t}(k)]^T$. The PEP between two codewords \mathbf{x} and \mathbf{y} can be determined by the codeword difference

¹We investigate the effect of relaxing this assumption on performance in Section 6. See also the work in [14].

matrix $\mathbf{B}(\mathbf{x}, \mathbf{y})$ [3, 4], where

$$\mathbf{B}(\mathbf{x}, \mathbf{y}) = \begin{pmatrix} \mathbf{x}_1(0) - \mathbf{y}_1(0) & \dots & \mathbf{x}_1(T-1) - \mathbf{y}_1(T-1) \\ \vdots & \vdots & \vdots \\ \mathbf{x}_{M_t}(0) - \mathbf{y}_{M_t}(0) & \dots & \mathbf{x}_{M_t}(T-1) - \mathbf{y}_{M_t}(T-1) \end{pmatrix}.$$

For fixed-rate codebook \mathcal{C} , the PEP between two distinct codewords \mathbf{x} and \mathbf{y} can be expressed as² [3]

$$(3) \quad P_e(\text{SNR}, \mathbf{x} \longrightarrow \mathbf{y}) \doteq \text{SNR}^{-M_r \text{rank}(\mathbf{B}(\mathbf{x}, \mathbf{y}))}.$$

Since we are dealing with a fixed-rate codebook, by using the simple union-bound argument, it can be shown that the diversity order d is given by [3]

$$(4) \quad d = M_r \min_{\mathbf{x} \neq \mathbf{y} \in \mathcal{C}} \text{rank}(\mathbf{B}(\mathbf{x}, \mathbf{y})).$$

The error probability is determined by *both* the coding gain and the diversity order. Hence, the code design criterion prescribed in [3] is to design the codebook \mathcal{C} so that the minimal rank of the codeword difference matrix corresponds to the required diversity order and the minimal determinant gives the corresponding coding gain. In this paper the focus is on the diversity order only.

2.3. Quaternions. We may view quaternions as a 4×4 matrix algebra over the real numbers \mathbf{R} , where right multiplication by the quaternion $q \stackrel{\text{def}}{=} q_0 + q_1i + q_2j + q_3k$ is described by

$$(5) \quad x_0 + x_1i + x_2j + x_3k \equiv \begin{bmatrix} x_0 & x_1 & x_2 & x_3 \end{bmatrix} \rightarrow \begin{bmatrix} x_0 & x_1 & x_2 & x_3 \end{bmatrix} \begin{bmatrix} q_0 & q_1 & q_2 & q_3 \\ -q_1 & q_0 & -q_3 & q_2 \\ -q_2 & q_3 & q_0 & -q_1 \\ -q_3 & -q_2 & q_1 & q_0 \end{bmatrix},$$

the conjugate quaternion \bar{q} is given by $\bar{q} \stackrel{\text{def}}{=} q_0 - q_1i - q_2j - q_3k$ and we have

$$(6) \quad q\bar{q} = \|q\|^2 = q_0^2 + q_1^2 + q_2^2 + q_3^2.$$

We may also view quaternions as pairs of complex numbers, where the product of quaternions (v, w) and (v', w') is given by

$$(7) \quad (v, w)(v', w') = (vv' - \bar{w}'w, vw' + \bar{v}'w)$$

²We use the notation \doteq to denote exponential equality, *i.e.*, $g(\text{SNR}) \doteq \text{SNR}^a$ means that $\lim_{\text{SNR} \rightarrow \infty} \frac{\log g(\text{SNR})}{\log \text{SNR}} = a$. Moreover, if $g(\text{SNR}) \doteq f(\text{SNR})$, it means that, $\lim_{\text{SNR} \rightarrow \infty} \frac{\log g(\text{SNR})}{\log \text{SNR}} = \lim_{\text{SNR} \rightarrow \infty} \frac{\log f(\text{SNR})}{\log \text{SNR}}$.

These are Hamilton's Biquaternions (see [16]), and right multiplication by the biquaternion (v, w) is described by

$$(8) \quad x_0 + x_1i + y_0j + y_1k \equiv \begin{bmatrix} x & y \end{bmatrix} \rightarrow \begin{bmatrix} x & y \end{bmatrix} \begin{bmatrix} v & w \\ -\bar{w} & \bar{v} \end{bmatrix}.$$

The matrices

$$\begin{bmatrix} 1 & 0 \\ 0 & 1 \end{bmatrix}; \begin{bmatrix} i & 0 \\ 0 & -i \end{bmatrix}; \begin{bmatrix} 0 & 1 \\ -1 & 0 \end{bmatrix}; \begin{bmatrix} 0 & i \\ i & 0 \end{bmatrix}$$

describe right multiplication by 1, i , j , and k , respectively. The matrix representing right multiplication by the biquaternion (v, w) is the 2×2 STBC introduced by Alamouti [6]. The columns of this matrix represent different time slots, the rows represent different antennas, and the entries are the symbols to be transmitted. Note that the rows and columns are orthogonal with respect to the standard inner product

$$(9) \quad \begin{bmatrix} x & y \end{bmatrix} \cdot \begin{bmatrix} x' & y' \end{bmatrix} = x\bar{x}' + y\bar{y}'.$$

There is a classical correspondence between unit quaternions and rotations in \mathbf{R}^3 given by

$$q \longrightarrow \mathbf{T}_q : p \longrightarrow \bar{q}pq$$

where we have identified vectors in \mathbf{R}^4 with quaternions $p = p_0 + p_1i + p_2j + p_3k$ [22]. The transformation \mathbf{T}_q fixes the real part $\Re(p)$ of the quaternion p , and if $q = q_0 + q_1i + q_2j + q_3k$, then \mathbf{T}_q describes rotation about the axis (q_1, q_2, q_3) through an angle 2θ where $\cos(\theta) = t$ and $\sin(\theta) = \sqrt{q_1^2 + q_2^2 + q_3^2}$.

EXAMPLE. The 16 quaternions $q = (\pm 1 \pm i \pm j \pm k)/2$ determine 8 symmetries of the unit cube with vertices $(\pm 1, \pm 1, \pm 1)/2$. The transformations \mathbf{T}_q divide into 4 sets $(\pm q, \pm \bar{q})$, each associated with an axis connecting opposite vertices. The two transformations \mathbf{T}_q in each set describe 120° rotation about this axis.

The 8 transformation \mathbf{T}_q are listed below together with their effect on i , j , and k

$$\begin{aligned} 1.) \quad q = \pm(1 + i + j + k)/2 \quad ; \quad \mathbf{T}_q = & \begin{bmatrix} 1 & 0 & 0 & 0 \\ 0 & 0 & 0 & 1 \\ 0 & 1 & 0 & 0 \\ 0 & 0 & 1 & 0 \end{bmatrix} \quad ; \quad \begin{array}{l} i \rightarrow k \\ j \rightarrow i \\ k \rightarrow j \end{array} \\ 2.) \quad q = \pm(1 - i - j - k)/2 \quad ; \quad \mathbf{T}_q = & \begin{bmatrix} 1 & 0 & 0 & 0 \\ 0 & 0 & 1 & 0 \\ 0 & 0 & 0 & 1 \\ 0 & 1 & 0 & 0 \end{bmatrix} \quad ; \quad \begin{array}{l} i \rightarrow j \\ j \rightarrow k \\ k \rightarrow i \end{array} \\ 3.) \quad q = \pm(1 + i - j - k)/2 \quad ; \quad \mathbf{T}_q = & \begin{bmatrix} 1 & 0 & 0 & 0 \\ 0 & 0 & 0 & -1 \\ 0 & -1 & 0 & 0 \\ 0 & 0 & 1 & 0 \end{bmatrix} \quad ; \quad \begin{array}{l} i \rightarrow -k \\ j \rightarrow -i \\ k \rightarrow j \end{array} \end{aligned}$$

$$\begin{aligned}
4.) \quad q = \pm(1 - i + j + k)/2 \quad ; \quad \mathbf{T}_q &= \begin{bmatrix} 1 & 0 & 0 & 0 \\ 0 & 0 & -1 & 0 \\ 0 & 0 & 0 & 1 \\ 0 & -1 & 0 & 0 \end{bmatrix} \quad ; \quad \begin{array}{l} i \rightarrow -j \\ j \rightarrow k \\ k \rightarrow -i \end{array} \\
5.) \quad q = \pm(1 - i + j - k)/2 \quad ; \quad \mathbf{T}_q &= \begin{bmatrix} 1 & 0 & 0 & 0 \\ 0 & 0 & 0 & 1 \\ 0 & -1 & 0 & 0 \\ 0 & 0 & -1 & 0 \end{bmatrix} \quad ; \quad \begin{array}{l} i \rightarrow k \\ j \rightarrow -i \\ k \rightarrow -j \end{array} \\
6.) \quad q = \pm(1 + i - j + k)/2 \quad ; \quad \mathbf{T}_q &= \begin{bmatrix} 1 & 0 & 0 & 0 \\ 0 & 0 & -1 & 0 \\ 0 & 0 & 0 & -1 \\ 0 & 1 & 0 & 0 \end{bmatrix} \quad ; \quad \begin{array}{l} i \rightarrow -j \\ j \rightarrow -k \\ k \rightarrow i \end{array} \\
7.) \quad q = \pm(1 - i - j + k)/2 \quad ; \quad \mathbf{T}_q &= \begin{bmatrix} 1 & 0 & 0 & 0 \\ 0 & 0 & 0 & -1 \\ 0 & 1 & 0 & 0 \\ 0 & 0 & -1 & 0 \end{bmatrix} \quad ; \quad \begin{array}{l} i \rightarrow -k \\ j \rightarrow i \\ k \rightarrow -j \end{array} \\
8.) \quad q = \pm(1 + i + j - k)/2 \quad ; \quad \mathbf{T}_q &= \begin{bmatrix} 1 & 0 & 0 & 0 \\ 0 & 0 & 1 & 0 \\ 0 & 0 & 0 & -1 \\ 0 & -1 & 0 & 0 \end{bmatrix} \quad ; \quad \begin{array}{l} i \rightarrow j \\ j \rightarrow -k \\ k \rightarrow -i \end{array}
\end{aligned}$$

Note that the odd-numbered transformations \mathbf{T}_q map $i \rightarrow \pm k$; $k \rightarrow \pm j$; $j \rightarrow \pm i$ while the even-numbered ones map $i \rightarrow \pm j$; $j \rightarrow \pm k$; $k \rightarrow \pm i$. In both cases, the product of the signs is equal to 1. See Appendix A for more information on the transformation \mathbf{T}_q .

2.4. Correspondence Between Quaternions and Matrices. There is an isomorphism between the quaternions q and 4×4 real matrices or 2×2 complex matrices in the following way

$$(10) \quad q \cong \begin{bmatrix} q_0 & q_1 & q_2 & q_3 \\ -q_1 & q_0 & -q_3 & q_2 \\ -q_2 & q_3 & q_0 & -q_1 \\ -q_3 & -q_2 & q_1 & q_0 \end{bmatrix} \cong \begin{bmatrix} q^c(0) & q^c(1) \\ -\bar{q}^c(1) & \bar{q}^c(0) \end{bmatrix} = \mathbf{Q}$$

where $q^c(0), q^c(1) \in \mathbf{C}$, and $q^c(0) = q_0 + iq_1$, $q^c(1) = q_2 + iq_3$. Therefore, we can interchangeably use the matrix representation for the quaternions in order to demonstrate properties. We will represent the 2×2 complex version of q by \mathbf{Q} . We will define norms as,

$$(11) \quad \|\mathbf{Q}\|^2 = \|q\|^2 = q_0^2 + q_1^2 + q_2^2 + q_3^2 = |q^c(0)|^2 + |q^c(1)|^2.$$

3. A New Quaternionic Space-Time Block Code. We consider the space-time block code

$$\begin{bmatrix} p & q \\ -\bar{q} & \frac{\bar{q}p q}{\|q\|^2} \end{bmatrix}$$

where the entries are quaternions. We may replace the quaternions p and q by the corresponding Alamouti 2×2 blocks to obtain a 4×4 STBC with complex entries.

$$(12) \quad \begin{bmatrix} \mathbf{P} & \mathbf{Q} \\ -\bar{\mathbf{Q}} & \frac{\bar{\mathbf{Q}}\mathbf{P}\mathbf{Q}}{\|\mathbf{Q}\|^2} \end{bmatrix} \begin{bmatrix} \bar{\mathbf{P}} & -\mathbf{Q} \\ \bar{\mathbf{Q}} & \frac{\bar{\mathbf{Q}}\mathbf{P}\mathbf{Q}}{\|\mathbf{Q}\|^2} \end{bmatrix} = (\|p\|^2 + \|q\|^2)\mathbf{I}.$$

Observe that the rows of this code are orthogonal with respect to the standard inner product operation. Since multiplication of quaternions is not commutative, it is not possible to have a 2×2 linear code over the quaternions with orthogonal rows and orthogonal columns [5]. We have abstracted the concept of a 2×2 code with orthogonal rows from the complex numbers to the quaternions. Note that if p and q were complex numbers rather than quaternions, then this code would collapse to the Alamouti STBC. In Appendix B, we prove that this code achieves maximum diversity order.

EXAMPLE. QPSK signaling corresponds to choosing the quaternions p and q from the set $(\pm 1 \pm i \pm j \pm k)/2$. In this case, there is **no constellation expansion** because $\frac{\bar{q}p q}{\|q\|^2}$ is always a quaternion of this same form.

4. Coherent Decoding.

4.1. Maximum Likelihood Decoding. We can represent the model in (1) by quaternionic algebra. For simplicity, let us consider $M_r = 1$; all arguments can be easily generalized to $M_r > 1$. Consider the 2×2 complex matrices formed as

$$(13) \quad \mathbf{R}_1 = \begin{bmatrix} \mathbf{r}(0) & \mathbf{r}(1) \\ -\bar{\mathbf{r}}(1) & \bar{\mathbf{r}}(0) \end{bmatrix}; \quad \mathbf{R}_2 = \begin{bmatrix} \mathbf{r}(2) & \mathbf{r}(3) \\ -\bar{\mathbf{r}}(3) & \bar{\mathbf{r}}(2) \end{bmatrix}$$

$$\mathbf{H}_1 = \begin{bmatrix} \mathbf{H}(1,1) & \mathbf{H}(1,2) \\ -\bar{\mathbf{H}}(1,2) & \bar{\mathbf{H}}(1,1) \end{bmatrix}; \quad \mathbf{H}_2 = \begin{bmatrix} \mathbf{H}(1,3) & \mathbf{H}(1,4) \\ -\bar{\mathbf{H}}(1,4) & \bar{\mathbf{H}}(1,3) \end{bmatrix}$$

where $\mathbf{H}(u, v)$ is the $(u, v)^{th}$ component of the channel matrix \mathbf{H} . Then we can rewrite (1) for our code as

$$(14) \quad \begin{bmatrix} \mathbf{R}_1 & \mathbf{R}_2 \end{bmatrix} = \begin{bmatrix} \mathbf{H}_1 & \mathbf{H}_2 \end{bmatrix} \begin{bmatrix} \mathbf{P} & \mathbf{Q} \\ -\bar{\mathbf{Q}} & \frac{\bar{\mathbf{Q}}\mathbf{P}\mathbf{Q}}{\|\mathbf{Q}\|^2} \end{bmatrix} + \begin{bmatrix} \mathbf{Z}_1 & \mathbf{Z}_2 \end{bmatrix}$$

where the noise vectors are also replaced by corresponding quaternionic matrices of the forms given in (13).

From (14), the ML decoding rule is given by³

$$\begin{aligned}
\{\hat{\mathbf{P}}, \hat{\mathbf{Q}}\} &= \arg \min_{\mathbf{P}, \mathbf{Q}} \left\| \begin{bmatrix} \mathbf{R}_1 & \mathbf{R}_2 \end{bmatrix} - \begin{bmatrix} \mathbf{H}_1 & \mathbf{H}_2 \end{bmatrix} \begin{bmatrix} \mathbf{P} & \mathbf{Q} \\ -\bar{\mathbf{Q}} & \frac{\mathbf{Q}\mathbf{P}\mathbf{Q}}{\|\mathbf{Q}\|^2} \end{bmatrix} \right\|^2 \\
(15) \quad &= \arg \max_{\mathbf{P}, \mathbf{Q}} \Re \left\{ \text{trace} \left(\begin{bmatrix} \mathbf{R}_1 & \mathbf{R}_2 \end{bmatrix} \begin{bmatrix} \bar{\mathbf{P}} & -\mathbf{Q} \\ \bar{\mathbf{Q}} & \frac{\mathbf{Q}\mathbf{P}\mathbf{Q}}{\|\mathbf{Q}\|^2} \end{bmatrix} \begin{bmatrix} \bar{\mathbf{H}}_1 \\ \bar{\mathbf{H}}_2 \end{bmatrix} \right) \right\}
\end{aligned}$$

4.2. Utilizing The Code Structure. We can write (14) in quaternionic algebra as follows

$$(16) \quad \begin{bmatrix} r_1 & r_2 \end{bmatrix} = \begin{bmatrix} h_1 & h_2 \end{bmatrix} \begin{bmatrix} p & q \\ -\bar{q} & \frac{\bar{q}\bar{p}q}{\|q\|^2} \end{bmatrix} + \begin{bmatrix} z_1 & z_2 \end{bmatrix},$$

where we have defined h_1, h_2 as the quaternions corresponding to the matrices $\mathbf{H}_1, \mathbf{H}_2$ given in (14). Consider the linear combining operation

$$\tilde{r}_1 \stackrel{def}{=} h_1 \bar{r}_1 + r_2 \bar{h}_2 = h_1 \bar{p} \bar{h}_1 + h_2 \left(\frac{\bar{q}\bar{p}q}{\|q\|^2} \right) \bar{h}_2 + \underbrace{h_1 \bar{z}_1 + z_2 \bar{h}_2}_{\tilde{z}_0}$$

so that

$$(17) \quad \Re(\tilde{r}_1) = \Re(h_1 \bar{r}_1 + r_2 \bar{h}_2) = (\|h_1\|^2 + \|h_2\|^2) p_0 + \Re(\tilde{z}_0)$$

which can be used to calculate p_0 by applying a hard slicer to the left hand side of (17). Now, from the first column of (16), we can write

$$\begin{aligned}
r_1 i &= h_1 p i - h_2 \bar{q} i + z_1 i \\
(18) \quad &\Rightarrow h_1 i \bar{r}_1 = h_1 (i \bar{p}) \bar{h}_1 - h_1 i \bar{q} \bar{h}_2 + h_1 i \bar{z}_1.
\end{aligned}$$

Next, consider the second column of (16). We have

$$\begin{aligned}
r_2 (i \mathbf{T}_q) &= r_2 \left(\frac{\bar{q} i q}{\|q\|^2} \right) = h_1 i q + h_2 \frac{\bar{q} \bar{p} i q}{\|q\|^2} + z_2 \frac{\bar{q} i q}{\|q\|^2} \\
(19) \quad &\Rightarrow r_2 (i \mathbf{T}_q) \bar{h}_2 = h_1 i q \bar{h}_2 + h_2 \frac{\bar{q} \bar{p} i q}{\|q\|^2} \bar{h}_2 + z_2 (i \mathbf{T}_q) \bar{h}_2.
\end{aligned}$$

Adding (18) and (19) and taking the real part, we get

$$\begin{aligned}
\Re(\tilde{r}_2) &\stackrel{def}{=} \Re(h_1 i \bar{r}_1 + r_2 (i \mathbf{T}_q) \bar{h}_2) = \Re(h_1 (i \bar{p}) \bar{h}_1 + h_2 \frac{\bar{q} \bar{p} i q}{\|q\|^2} \bar{h}_2 + \underbrace{h_1 i \bar{z}_1 + z_2 (i \mathbf{T}_q) \bar{h}_2}_{\tilde{z}_1}) \\
(20) \quad &= (\|h_1\|^2 + \|h_2\|^2) p_1 + \Re(\tilde{z}_1).
\end{aligned}$$

³Assuming that $\|\mathbf{P}\|$ and $\|\mathbf{Q}\|$ are constant.

Similarly, we can show that

$$\begin{aligned}
 \Re(\tilde{r}_3) &\stackrel{def}{=} \Re(h_1 j \bar{r}_1 + r_2 (j \mathbf{T}_q) \bar{h}_2) = \Re(h_1 (j \bar{p}) \bar{h}_1 + h_2 \frac{\bar{q} \bar{p} j q}{\|q\|^2} \bar{h}_2 + \underbrace{h_1 j \bar{z}_1 + z_2 (j \mathbf{T}_q) \bar{h}_2}_{\tilde{z}_2}) \\
 (21) \qquad &= (\|h_1\|^2 + \|h_2\|^2) p_2 + \Re(\tilde{z}_2)
 \end{aligned}$$

$$\begin{aligned}
 \text{and } \Re(\tilde{r}_4) &\stackrel{def}{=} \Re(h_1 k \bar{r}_1 + r_2 (k \mathbf{T}_q) \bar{h}_2) = \Re(h_1 (k \bar{p}) \bar{h}_1 + h_2 \frac{\bar{q} \bar{p} k q}{\|q\|^2} \bar{h}_2 + \underbrace{h_1 k \bar{z}_1 + z_2 (k \mathbf{T}_q) \bar{h}_2}_{\tilde{z}_3}) \\
 (22) \qquad &= (\|h_1\|^2 + \|h_2\|^2) p_3 + \Re(\tilde{z}_3) .
 \end{aligned}$$

Decoding proceeds as follows. First p_0 is calculated by applying a hard slicer to the left hand side of (17). Next, as shown in Section 2.3, there are 8 choices for the transformation \mathbf{T}_q where each can be used to calculate a candidate for the triplet (p_1, p_2, p_3) by applying a hard slicer to the left hand sides of Equations (20)-(22). For each choice of \mathbf{T}_q , there are 2 choices of q (sign ambiguity). Finally, the 16 candidates for (p, q) are compared using the ML metric in (15) to obtain the decoded QPSK information symbols. We show in Appendix C that the statistics $\Re(\tilde{r}_1)$ through $\Re(\tilde{r}_4)$ are *sufficient* for ML decoding. In addition, we emphasize that there is no loss of optimality in applying the hard QPSK slicer operation to (17), (20)-(22) since the noise samples are zero-mean uncorrelated Gaussian.

We conclude this section with the following two remarks. First, we can think of the linear-combining operations in (17) and (20)-(22) as the generalization of standard Alamouti STBC decoding to our 4×4 quaternionic STBC. Second, with 2 receive antennas, ML decoding proceeds by applying the combining operations in (17) and (20)-(22) to each receive antenna and then adding the respective signals to generate 4 signals which are used to decode (p, q) as in the single-antennas case described above.

5. Differential Encoding and Decoding. In some circumstances, it is desirable to forgo the channel estimation module to keep the receiver complexity low. Under such circumstances, differential decoding algorithms become attractive despite their SNR loss from coherent decoding. In this section, we develop the differential encoding and decoding algorithm for our quaternionic code.

Our starting point is the input-output relationship in (16) which can be written in compact matrix notation as follows

$$(23) \qquad \mathbf{r}^{(k)} = \mathbf{h} \mathbf{C}^{(k)} + \mathbf{z}^{(k)} .$$

Consider the following differential encoding rule

$$(24) \qquad \mathbf{C}^{(k)} = \mathbf{C}^{(k-1)} \mathbf{U}^{(k)}$$

where the information matrix $\mathbf{U}^{(k)} = \begin{bmatrix} \mathbf{P} & \mathbf{Q} \\ -\bar{\mathbf{Q}} & \frac{\bar{\mathbf{Q}} \mathbf{P} \mathbf{Q}}{\|q\|^2} \end{bmatrix}$. Therefore, we have

$$(25) \qquad \mathbf{r}^{(k)} = \mathbf{h} \mathbf{C}^{(k-1)} \mathbf{U}^{(k)} + \mathbf{z}^{(k)}$$

from which we can write

$$\begin{aligned}
 \mathbf{r}^{(k)} &= (\mathbf{r}^{(k-1)} - \mathbf{z}^{(k-1)})\mathbf{U}^{(k)} + \mathbf{z}^{(k)} \\
 (26) \qquad &= \mathbf{r}^{(k-1)}\mathbf{U}^{(k)} + \underbrace{\mathbf{z}^{(k)} - \mathbf{z}^{(k-1)}\mathbf{U}^{(k)}}_{\tilde{\mathbf{z}}^{(k)}}.
 \end{aligned}$$

This equation has identical form to the received signal equation in the coherent case **except** for 2 main differences

- The previous output vector $\mathbf{r}^{(k-1)}$ in (26) plays the role of the channel coefficient vector and is known at the receiver.
- Since $\mathbf{U}^{(k)}$ is a **Unitary** matrix by construction, the equivalent noise vector $\tilde{\mathbf{z}}^{(k)}$ will also be zero-mean white Gaussian (like $\mathbf{z}^{(k)}$ and $\mathbf{z}^{(k-1)}$) but with *twice* the variance.

Hence, the same efficient ML coherent decoding algorithm applies in the differential case as well but at an additional 3 dB performance penalty at high SNR.

6. Simulation Results. In this section, we present simulation results on the performance of our proposed STBC with the efficient ML decoding algorithm. We assume QPSK modulation, a single antenna at the receiver (unless otherwise states), and no channel state information (CSI) at the transmitter.

We start by investigating the resulting performance degradation when the assumption of perfect CSI at the receiver is not satisfied. We consider two scenarios. In the first scenario, no CSI is available at the receiver and the differential encoding/decoding scheme of Section 5 is used. Figure 5 shows the SNR penalty from coherent decoding (with perfect CSI) is 3 dB at high SNR. In the second scenario, the coherent ML decoder uses estimated CSI acquired by transmitting a pilot codeword of the same quaternionic structure and using a simple matched filter operation at the receiver to calculate the CSI vector. Figure 6 shows that the performance loss due to channel estimation is about 2-3 dB which is comparable to the differential technique. Next, we compare the performance of both scheme in a time-varying channel. The pilot-based channel estimation scheme will suffer performance degradation since the channel estimate will be outdated due to the Doppler effect. To mitigate this effect, we need to increase the frequency of pilot codeword insertion as the Doppler frequency increases which in turn increases the training overhead. We assume a fixed pilot insertion rate of one every 20 codewords; i.e. a training overhead of only 5%. Similarly, the differential scheme will also suffer performance degradation since the assumption of a constant channel over 2 consecutive codewords (i.e. 8 symbol intervals) is no longer valid. Figure 7 shows that for high mobile speeds (high Doppler), an error floor occurs for both schemes. Both schemes achieve comparable performance for low (pedestrian) speeds but the pilot-based scheme performs better at moderate to high speeds at the expense of a more complex receiver (to perform channel estimation) and the pilot transmission overhead.

Figure 8 depicts the significant additional performance improvement achievable by adding a second receive antenna (resulting in 8-th order diversity) and using the receiver combining rules described in Section 4.2. Figure 9 shows that the proposed code achieves a lower bit error rate than the full-rate quasi-orthogonal design [13] at high SNR since it achieves a diversity order for 2.

Next, we compare the performance of our proposed quaternionic code with the following rate- $\frac{1}{2}$ and rate- $\frac{3}{4}$ orthogonal designs [5]

$$(27) \quad \mathbf{G}_1 = \begin{bmatrix} x_1 & x_2 & x_3 & x_4 \\ -x_2 & x_1 & -x_4 & x_3 \\ -x_3 & x_4 & x_1 & -x_2 \\ -x_4 & -x_3 & x_2 & x_1 \\ \bar{x}_1 & \bar{x}_2 & \bar{x}_3 & \bar{x}_4 \\ -\bar{x}_2 & \bar{x}_1 & -\bar{x}_4 & \bar{x}_3 \\ -\bar{x}_3 & \bar{x}_4 & \bar{x}_1 & -\bar{x}_2 \\ -\bar{x}_4 & -\bar{x}_3 & \bar{x}_2 & \bar{x}_1 \end{bmatrix}; \quad \mathbf{G}_2 = \begin{bmatrix} x_1 & x_2 & x_3 & 0 \\ -\bar{x}_2 & \bar{x}_1 & 0 & x_3 \\ \bar{x}_3 & 0 & -\bar{x}_1 & x_2 \\ 0 & \bar{x}_3 & -\bar{x}_2 & -x_1 \end{bmatrix}.$$

In order to make a fair comparison, all codes are normalized to unit transmit energy. Figure 10 shows that our proposed STBC with QPSK modulation achieves lower frame error rate (FER) than the rate- $\frac{1}{2}$ orthogonal design with 16-QAM modulation at the same transmission spectral efficiency of 2 bits per channel use (PCU). We cannot find any signal constellation for the rate- $\frac{3}{4}$ orthogonal design (Octonion) that would make its spectral efficiency equal to that of the proposed STBC. Therefore, we compare both codes in Figure 11 based on the Effective Throughput η defined as $\eta = (1 - FER) * R * \log_2(M)$, where M is the constellation size. We assume a frame to be in error if any information bit in the frame is decoded incorrectly. A frame in error is not considered for retransmission and is simply discarded from the queue. We assume QPSK modulation for both coding schemes and 240 information bits per frame. The figure shows that at high SNR (FER near zero), our proposed code achieves a throughput level of 2 bits PCU whereas the achievable throughput for the Octonion is 1.5 bits PCU. We can observe a cross-over point at 13 dB which is attributed to the fact that the constant transmit energy is distributed equally over 4 symbols for our STBC and only over 3 symbols in the Octonion. By concatenating both STBC's with an outer RS(15, 11) code, the cross-over point shifts to around 8 dB, as depicted in Figure 12. The RS code overhead is included in the calculated throughput.

Finally, we investigate the performance of our proposed code in a frequency-selective fading channel. As an example, we consider the broadband wireless access application as in the IEEE 802.16 standard (WiMAX). We assume the widely-used Stanford University Interim (SUI) channel models [20] where each of the three-tap SUI channel models is defined for a particular terrain type with varying degree of Ricean fading \mathbf{K} factors and Doppler frequency. We combine our quaternionic STBC

with Orthogonal Frequency Division Multiplexing (OFDM) transmission where each codeword is now transmitted over four consecutive OFDM symbol durations (for each subcarrier). In our simulations, we use 256 sub-carriers and a cyclic prefix length of 64 samples. We simultaneously transmit 256 codewords from four transmit antennas over four OFDM symbols and assume that the channel remains fixed over that period. We also use a RS(255, 163) outer code and frequency-interleave the coded data before transmitting through the channel. Figure 13 illustrates the significant performance gains achieved by our proposed 4-TX STBC in the 802.16 environment as compared to SISO transmission. To put these SNR gains in perspective, at BER= 10^{-3} , these SNR gains translate to a 50% increase in the cell coverage area assuming 1 receive Antenna. By adding a second receive antenna, the percentage increase becomes 166%⁴.

7. Conclusions. We used the mathematical theory of quaternions to design and analyze a novel Rate-1, full-diversity, orthogonal STBC for 4 transmit antennas and complex signal constellations. Establishing the connection to quaternions allowed to derive several key results analytically including full diversity for any M -PSK constellation, no constellation expansion for QPSK, and a low-complexity ML coherent decoding algorithm. We generalized our results to the case of multiple receive antennas and to differential decoding. A detailed investigation on the application of our proposed STBC to the WiMAX application demonstrated a 50% and 166% increase in the cell coverage area when combined with 1 and 2 receive antenna(s) respectively, at BER= 10^{-3} compared with the single-transmit-antenna case.

Appendix A. Finite Groups of Rotations in \mathbf{R}^3 and Unit Quaternions.

If $q = a + bi + cj + dk$ is a quaternion, then the matrices

$$(28) \quad q_L = \begin{bmatrix} a & -b & -c & -d \\ b & a & -d & c \\ c & d & a & -b \\ d & -c & b & a \end{bmatrix}; \quad q_R = \begin{bmatrix} a & -b & -c & -d \\ b & a & d & -c \\ c & -d & a & b \\ d & c & -b & a \end{bmatrix}$$

describe left and right multiplication by q . The 2:1 correspondence between unit quaternions ($a^2 + b^2 + c^2 + d^2 = 1$) and rotations in \mathbf{R}^3 is given by $q \longrightarrow T_q = \bar{q}_L q_R$ where $\bar{q} = a - bi - cj - dk$. The next theorem classifies finite groups of rotations in \mathbf{R}^3 (a proof can be found in Chapter 5 of [23]).

THEOREM A.1.

Every finite subgroup of rotations in \mathbf{R}^3 is one of the following:

⁴These calculations assume a path loss exponent of 4 which is recommended for the SUI-3 channel model with a Base Station height of 50 meters [20].

1. the cyclic group C_k of rotations by multiples of $\frac{2\pi}{k}$ about a line;
2. the dihedral group D_k of symmetries of a regular k -gon;
3. the tetrahedral group T (isomorphic to the alternating group A_4);
4. the octahedral group O (isomorphic to the symmetric group S_4);
5. the icosahedral group I (isomorphic to A_5)

We denote the inverse images of these groups under the 2:1 correspondence by $2C_k$, $2D_k$, $2T$, $2O$, and $2I$ respectively. These are the finite groups of quaternions containing ± 1 (Chapters 1, 2 and 3 of [22] contain more information about these groups).

We focus on the octahedral group O which is the symmetry group of the unit cube with vertices $(\pm 1, \pm 1, \pm 1)$ as shown in Figure 1.

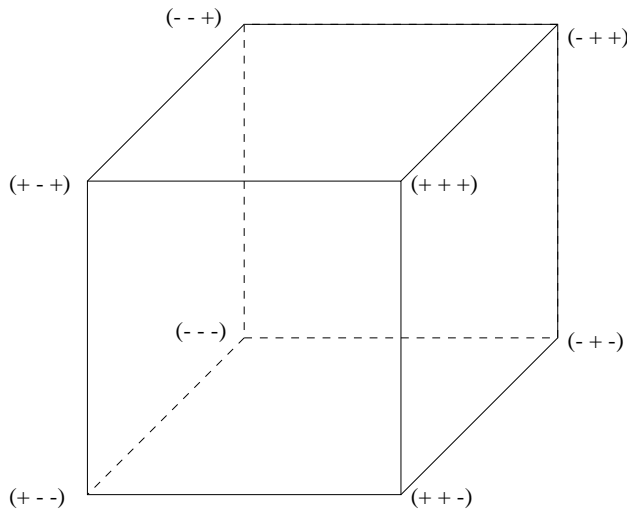


FIG. 1. The unit cube.

We label the body diagonals of the unit cube as follows: (1)(+++ , ---); (2)(- + + , + - -); (3)(- - + , + + -); and (4)(+ - + , - + -). These diagonals are permuted by the octahedral group, and this representation provides the isomorphism with the symmetric group S_4 . Table 1 connects conjugacy classes in S_4 with unit quaternions q and a geometric description of corresponding rotation T_q .

The 4×4 space-time code is given by

$$\begin{bmatrix} p & q \\ -\bar{q} & \bar{q}\bar{p}q \end{bmatrix}$$

where each unit quaternion entry is realized as a 2×2 Alamouti matrix with complex entries. If $p, q \in 2O$, then these complex entries are drawn from the constellation shown in Figure 2.

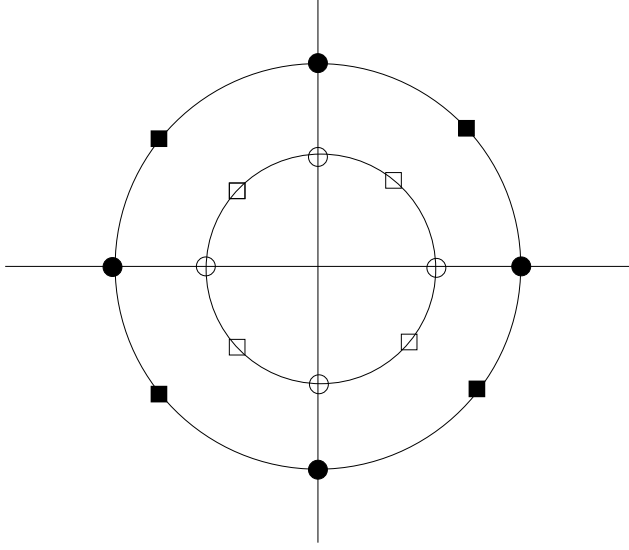


FIG. 2. Inventory of possible complex entries for the space-time code.

TABLE 1

Symmetries of the unit cube organized by conjugacy class.

Conjugacy Class in S_4	Unit Quaternions q	Rotations $T_q = \bar{q}_L q_R$
identity	± 1	identity
double transpositions	$\pm i, \pm j, \pm k$	rotation through π about the x, y and z axis
3-cycles	$\frac{(\pm 1 \pm i \pm j \pm k)}{2}$	rotation through $\frac{2\pi}{3}$ about a body diagonal
4-cycles	$\frac{\pm 1 \pm i}{\sqrt{2}}, \frac{\pm 1 \pm j}{\sqrt{2}}, \frac{\pm 1 \pm k}{\sqrt{2}}$	rotation through $\frac{\pi}{2}$ about the x, y and z axis
transpositions	$\frac{\pm i \pm j}{\sqrt{2}}, \frac{\pm i \pm k}{\sqrt{2}}, \frac{\pm j \pm k}{\sqrt{2}}$	rotation through π about the line connecting the midpoints of opposite sides

This algebraic framework enables the construction of new codes. For example, Table 2 shows how to select unit quaternions p and q to construct a rate $\frac{9}{4}$ code for 8-PSK (the inner constellation) with full-diversity.

Appendix B. Full Diversity Proof.

In this paper, we define a QPSK symbol to be of the form $x_l = \frac{1}{\sqrt{2}} e^{j \frac{\pi}{4} (2k+1)}$ for $k = 0, 1, 2, 3$.

We need to verify that given two different space-time codewords, say $\mathbf{C}_{p,q}$ and $\mathbf{C}_{p',q'}$, the difference $\mathbf{C}_{p,q} - \mathbf{C}_{p',q'}$ is nonsingular. Now

$$(29) \quad \mathbf{C}_{p,q} - \mathbf{C}_{p',q'} = \begin{bmatrix} p - p' & q - q' \\ -(\bar{q} - \bar{q}') & \frac{\bar{q}p q}{\|q\|^2} - \frac{\bar{q}' p' q'}{\|q'\|^2} \end{bmatrix}$$

TABLE 2

Codewords in a rate- $\frac{9}{4}$ space-time code for 8PSK. The 9 input bits choose one of 32 unit quaternions q and one of 16 unit quaternions p

Unit Quaternion	Pair of Complex Entries in Constituent Alamouti Matrix	Number of Choices
$p = \frac{(\pm 1 \pm i \pm j \pm k)}{2}$	\square, \square	16
$q = \frac{(\pm 1 \pm i \pm j \pm k)}{2}$	\square, \square	16
$q = \frac{(\pm 1 \pm j)}{\sqrt{2}}, \frac{(\pm 1 \pm k)}{\sqrt{2}}, \frac{(\pm i \pm j)}{\sqrt{2}}, \frac{(\pm i \pm k)}{\sqrt{2}}$	\circ, \circ	16

and by applying a similarity transformation

$$\begin{bmatrix} \frac{\bar{l}}{\|l\|} & 0 \\ 0 & \frac{\bar{m}}{\|m\|} \end{bmatrix} (\mathbf{C}_{p,q} - \mathbf{C}_{p',q'}) \begin{bmatrix} \frac{l}{\|l\|} & 0 \\ 0 & \frac{m}{\|m\|} \end{bmatrix}$$

we may replace p , p' , q , and q' by $\frac{\bar{l}pl}{\|l\|^2}$, $\frac{\bar{l}p'l}{\|l\|^2}$, $\frac{\bar{l}qm}{\|l\|\|m\|}$, and $\frac{\bar{l}q'm}{\|l\|\|m\|}$, respectively.

We apply an elementary row operation to (29) to obtain

$$\begin{bmatrix} p - p' & q - q' \\ 0 & \frac{\|q - q'\|^2}{\|p - p'\|^2} \frac{(\bar{q} - \bar{q}')(\bar{p} - \bar{p}')(q - q')}{\|q - q'\|^2} + \frac{\bar{q}\bar{p}q}{\|q\|^2} - \frac{\bar{q}'\bar{p}'q'}{\|q'\|^2} \end{bmatrix}$$

We now take $l = 1$, $m = \bar{q} - \bar{q}'$, so that $q - q'$ is real. This means that the rotations determined by q and q' share the same axis and that

$$\frac{(\bar{q} - \bar{q}')(\bar{p} - \bar{p}')(q - q')}{\|q - q'\|^2} = \bar{p} - \bar{p}'$$

We need to show that if $p \neq p'$ then

$$\frac{\|q - q'\|^2}{\|p - p'\|^2} (\bar{p} - \bar{p}') + \frac{\bar{q}\bar{p}q}{\|q\|^2} - \frac{\bar{q}'\bar{p}'q'}{\|q'\|^2} \neq 0$$

This turns out to be true when $\|p\| = \|p'\| = \|q\| = \|q'\|$.

THEOREM B.1.

If $\|p\| = \|p'\| = \|q\| = \|q'\|$, then the quaternionic space-time code has full diversity.

We suppose that

$$(30) \quad \frac{\|q - q'\|^2}{\|p - p'\|^2} (\bar{p} - \bar{p}') + \frac{\bar{q}\bar{p}q}{\|q\|^2} - \frac{\bar{q}'\bar{p}'q'}{\|q'\|^2} = 0.$$

If x_{\Re} is the real part of a quaternion x , then (30) implies

$$(31) \quad \frac{\|q - q'\|^2}{\|p - p'\|^2} (\bar{p} - \bar{p}')_{\Re} + (\bar{p} - \bar{p}')_{\Re} = 0.$$

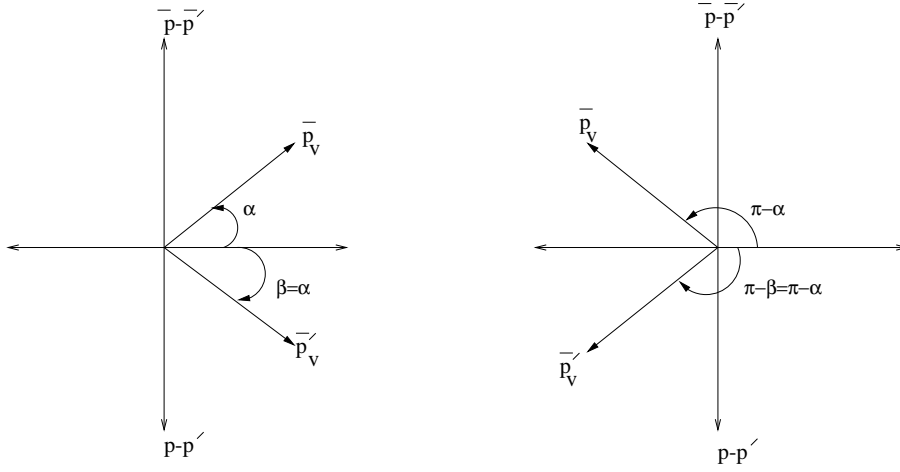
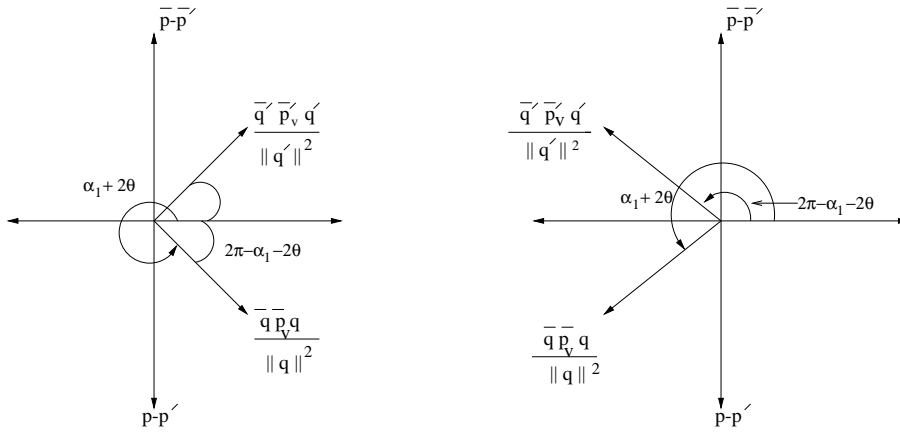
FIG. 3. The geometry of projections \bar{p}_V and \bar{p}'_V .

FIG. 4. The geometry of the rotated projections.

It follows that $(\bar{p} - \bar{p}')_{\Re} = 0$, so that $(p - p')$ is pure imaginary.

Next we project each term in (30) onto the common axis A of the rotations determined by q and q' to obtain

$$(32) \quad \frac{\|q - q'\|^2}{\|p - p'\|^2} (\bar{p} - \bar{p}')_A + \bar{p}_A - \bar{p}'_A = 0$$

It follows that $(\bar{p} - \bar{p}')_A = 0$, so that $(\bar{p} - \bar{p}')$ lies in the 2-dimensional real space $V = \langle (1000), A \rangle^\perp$. We scale the axis A so that it has norm 1, and we write q and q' in the form

$$\begin{aligned} q &= \|q\| \cos \theta + (\|q\| \sin \theta) A \\ q' &= \|q'\| \cos \phi + (\|q'\| \sin \phi) A \end{aligned}$$

where $0 \leq \theta, \phi < \pi$. Since $\|q\| = \|q'\|$, and since $(q - q')$ is real, we have $\theta = \phi$ or $\theta = \pi - \phi$.

If $\theta = \phi$ then $q = q'$ and it is clear that (29) is nonsingular. Therefore, we may suppose $\theta = \pi - \phi$, so that

$$(33) \quad \begin{aligned} q &= \|q\|\cos\theta + (\|q\|\sin\theta)A \\ q' &= -\|q\|\cos\theta + (\|q\|\sin\theta)A \end{aligned}$$

The quaternion q determines rotations through 2θ about the axis A , and the quaternion q' determines rotation through -2θ about the same axis.

If $p \neq p'$ then we may take $(\bar{p} - \bar{p}')$ to be a coordinate axis in the plane V . Let x_V be the projection of the quaternion x onto the plane V . Since $\|p\| = \|p'\|$, we have

$$\|p_V\|^2 = \|p\|^2 - \|p_{\Re}\|^2 - \|p_A\|^2 = -\|p'\|^2 - \|p'_{\Re}\|^2 - \|p'_A\|^2 = \|p'_V\|^2$$

and we consider the two geometries shown in Figure 3.

In either case,

$$\|\bar{p} - \bar{p}'\| = 2\|p_V\|\sin\alpha$$

and it follows from (33) that

$$(34) \quad \frac{\|q - q'\|^2}{\|p - p'\|^2} \|\bar{p} - \bar{p}'\| = \frac{4\|q\|^2\cos^2\theta}{2\|p_V\|\sin\alpha}$$

Since $\bar{p}_{\Re} = \bar{p}'_{\Re}$ and since $\bar{p}_A = \bar{p}'_A$, we have

$$(35) \quad \frac{\bar{q}\bar{p}q}{\|q\|^2} - \frac{\bar{q}'\bar{p}'q'}{\|q'\|^2} = \frac{\bar{q}\bar{p}_Vq}{\|q\|^2} - \frac{\bar{q}'\bar{p}'_Vq'}{\|q'\|^2}$$

It follows from (30) that the right hand side of (35) is a positive multiple of $p - p'$. Setting $\alpha_1 = \alpha$ or $\pi - \alpha$ according to the geometry in Figure 3, we need only consider the two geometries shown in Figure 4. Note that in either case $\sin(\alpha_1 + 2\theta) < 0$.

We observe that the angle between the two projections is $4\pi - 2\alpha_1 - 4\theta$ (equivalently $2\alpha_1 + 4\theta - 2\pi$), so that

$$\left\| \frac{\bar{q}\bar{p}_Vq}{\|q\|^2} - \frac{\bar{q}'\bar{p}'_Vq'}{\|q'\|^2} \right\| = 2|\sin(\alpha_1 + 2\theta)|\|p_V\|$$

Since $\sin(\alpha_1 + 2\theta) < 0$, we have $\sin(\alpha_1 + 2\theta - \pi) > 0$ and (30) implies

$$\begin{aligned} 4\|q\|^2\cos^2\theta - 4\sin\alpha_1\sin(\alpha_1 - \pi + 2\theta)\|p_V\|^2 &= 0 \\ 4\|q\|^2\cos^2\theta - 4\sin(\pi - \alpha_1)\sin(\alpha_1 - \pi + 2\theta)\|p_V\|^2 &= 0 \\ 4\|q\|^2\cos^2\theta - 2(\cos 2\theta - \cos 2(\alpha_1 - \pi + \theta))\|p_V\|^2 &= 0 \\ 4(\|q\|^2 - \|p_V\|^2)\cos^2\theta + 2(1 + \cos 2(\alpha_1 - \pi + \theta))\|p_V\|^2 &= 0 \end{aligned}$$

This is a contradiction since both terms are non-negative.

Appendix C. ML Optimality of the Reduced-Complexity Decoder.

In this section we will prove the ML optimality of the proposed reduced-complexity decoding algorithm presented in Section 4. We will start by showing that there is a unique correspondence between the 2 sets of variables $\{\tilde{r}_i\}$ and $\{r_i\}$ for $i = 1, \dots, 4$. We will also show that only the real part of $\{\tilde{r}_i\}$ contains relevant information for the decoder. The one-to-one mapping between $\{\tilde{r}_i\}$ and $\{r_i\}$ and the information sufficiency in the real part of $\{\tilde{r}_i\}$ guarantee that the proposed reduced-complexity decoding scheme is ML optimum and there is no loss of information in the proposed pre-processing stage.

We start with Equations (17) and (20)-(22) for \tilde{r}_i where $i = 1, \dots, 4$. To simplify notation, we omit the additive noise term for the remaining part of this appendix and get

$$\begin{aligned}\tilde{r}_1 &= h_1 \bar{r}_1 + r_2 \bar{h}_2 \\ \tilde{r}_2 &= h_1 i \bar{r}_1 + r_2 (\bar{q} i q) \bar{h}_2 \\ \tilde{r}_3 &= h_1 j \bar{r}_1 + r_2 (\bar{q} j q) \bar{h}_2 \\ \tilde{r}_4 &= h_1 k \bar{r}_1 + r_2 (\bar{q} k q) \bar{h}_2\end{aligned}$$

The above set of equations, after left multiplication by \bar{h}_1 , $-i\bar{h}_1$, $-j\bar{h}_1$, and $-k\bar{h}_1$, respectively, are expressed as

$$\begin{aligned}\bar{h}_1 \tilde{r}_1 &= \bar{r}_1 + \bar{h}_1 r_2 \bar{h}_2 \\ -i\bar{h}_1 \tilde{r}_2 &= \bar{r}_1 - i\bar{h}_1 r_2 (\bar{q} i q) \bar{h}_2 \\ -j\bar{h}_1 \tilde{r}_3 &= \bar{r}_1 - j\bar{h}_1 r_2 (\bar{q} j q) \bar{h}_2 \\ -k\bar{h}_1 \tilde{r}_4 &= \bar{r}_1 - k\bar{h}_1 r_2 (\bar{q} k q) \bar{h}_2\end{aligned}$$

Next, we assume that there exist r'_1 and r'_2 , in addition to r_1 and r_2 , which can result in the same \tilde{r}_i for $i = 1, \dots, 4$ and check if we reach a contradiction. Let us define

$$\begin{aligned}d_1 &= r_1 - r'_1 \\ d_2 &= r_2 - r'_2\end{aligned}$$

We can rewrite the expressions for \tilde{r}_1 and \tilde{r}_2 in terms of d_1 and d_2 as follows ⁵

$$(36) \quad \bar{d}_1 + \bar{h}_1 d_2 \bar{h}_2 = 0$$

$$(37) \quad \bar{d}_1 - i\bar{h}_1 d_2 \bar{q} i q \bar{h}_2 = 0$$

⁵We chose to work with \tilde{r}_1 and \tilde{r}_2 ; however, any two of them can be used.

From (36) and (37), we have

$$\begin{aligned}
\bar{h}_1 d_2 \bar{h}_2 &= -i \bar{h}_1 d_2 \bar{q} i \bar{q} \bar{h}_2 \\
\implies \bar{h}_1 d_2 \bar{h}_2 h_2 &= -i \bar{h}_1 d_2 \bar{q} i \bar{q} \bar{h}_2 h_2 \\
&\implies \bar{h}_1 d_2 \bar{q} = -i \bar{h}_1 d_2 \bar{q} i \bar{q} \\
&\implies (\bar{h}_1 d_2 \bar{q}) i = i (\bar{h}_1 d_2 \bar{q})
\end{aligned}$$

Both i and $\bar{h}_1 d_2 \bar{q}$ are members of the non-commutative quaternionic group. This commutative property between i and $\bar{h}_1 d_2 \bar{q}$ can hold only if $\bar{h}_1 d_2 \bar{q}$ is a scalar constant which is a clear contradiction to our assumption that the information symbol q is randomly drawn from a set of 2×2 arrays of complex symbols, (a.k.a. quaternions). Therefore, the above equality can hold only if

$$\bar{h}_1 d_2 \bar{q} = 0$$

The intrinsic *non-zero* condition on \bar{h}_1 and \bar{q} leads to

$$\begin{aligned}
d_2 &= 0 \\
\implies r_2 &= r_2'
\end{aligned}$$

Therefore, we conclude that the mapping between the two set $\{\tilde{r}_i\}$ and $\{r_i\}$ for $i = 1, \dots, 4$ is one-to-one. To complete the proof, we need to show that processing only the real part of $\{\tilde{r}_i\}$ does not cause any loss of information. As an example, we will show next that $\Re(\tilde{r}_2) = \Re(h_1 i \bar{r}_1 + r_2 (\bar{q} i q) \bar{h}_2)$ contains sufficient information for the ML detection of p_1 .

From (20),

$$\tilde{r}_2 = h_1 (i \bar{p}) \bar{h}_1 + h_2 \frac{\bar{q} \bar{p} i q}{\|q\|^2} \bar{h}_2$$

where h_1 , h_2 , p and q are quaternions, and h_1 and h_2 comprise the channel realizations for antennas (1, 2) and (3, 4), respectively.

First Term :

$$\begin{aligned}
h_1 (i \bar{p}) \bar{h}_1 &= (h_{1,0} + h_{1,1} i + h_{1,2} j + h_{1,3} k) i (p_0 - p_1 i - p_2 j - p_3 k) (h_{1,0} - h_{1,1} i - h_{1,2} j - h_{1,3} k) \\
&= (h_{1,0} + h_{1,1} i + h_{1,2} j + h_{1,3} k) (p_1 + p_0 i + p_3 j - p_2 k) (h_{1,0} - h_{1,1} i - h_{1,2} j - h_{1,3} k) \\
&= \underbrace{[(h_{1,0} p_1 - h_{1,1} p_0 - h_{1,2} p_3 + h_{1,3} p_2)]}_{c_1} + \underbrace{[(h_{1,0} p_0 + h_{1,1} p_1 - h_{1,2} p_2 - h_{1,3} p_3)]}_{c_2} i + \\
&\quad \underbrace{[(h_{1,0} p_3 + h_{1,1} p_2 + h_{1,2} p_1 + h_{1,3} p_0)]}_{c_3} j + \underbrace{[(-h_{1,0} p_2 + h_{1,1} p_3 - h_{1,2} p_0 + h_{1,3} p_1)]}_{c_4} k \\
&\quad (h_{1,0} - h_{1,1} i - h_{1,2} j - h_{1,3} k) \\
&= (c_1 h_{1,0} + c_2 h_{1,1} + c_3 h_{1,2} + c_4 h_{1,3}) + (-c_1 h_{1,1} + c_2 h_{1,0} - c_3 h_{1,3} + c_4 h_{1,2}) i + \\
&\quad (-c_1 h_{1,2} + c_2 h_{1,3} + c_3 h_{1,0} - c_4 h_{1,1}) j + (-c_1 h_{1,3} - c_2 h_{1,2} + c_3 h_{1,1} + c_4 h_{1,0}) k.
\end{aligned}$$

Therefore, the real part of this first term is given by

$$\begin{aligned}
\Re(h_1(i\bar{p})\bar{h}_1) &= c_1h_{1,0} + c_2h_{1,1} + c_3h_{1,2} + c_4h_{1,3} \\
&= h_{1,0}p_1h_{1,0} - h_{1,1}p_0h_{1,0} - h_{1,2}p_3h_{1,0} + h_{1,3}p_2h_{1,0} + h_{1,0}p_0h_{1,1} + h_{1,1}p_1h_{1,1} \\
&\quad - h_{1,2}p_2h_{1,1} - h_{1,3}p_3h_{1,1} + h_{1,0}p_3h_{1,2} + h_{1,1}p_2h_{1,2} + h_{1,2}p_1h_{1,2} + h_{1,3}p_0h_{1,2} \\
&\quad - h_{1,0}p_2h_{1,3} + h_{1,1}p_3h_{1,3} - h_{1,2}p_0h_{1,3} + h_{1,3}p_1h_{1,3} \\
&= (h_{1,0}^2 + h_{1,1}^2 + h_{1,2}^2 + h_{1,3}^2)p_1 \\
&= \|h_1\|^2 p_1.
\end{aligned}$$

Similarly, by expanding the i , j and k parts of this first term, it can be easily verified that they do not contain any information about p_1 and hence are irrelevant for its ML detection.

Second Term :

$$\begin{aligned}
h_2 \frac{\bar{q}\bar{p}i q}{\|q\|^2} \bar{h}_2 &= [(h_{2,0} + h_{2,1}i + h_{2,2}j + h_{2,3}k)(q_0 - q_1i - q_2j - q_3k)(p_0 - p_1i - p_2j - p_3k)i \\
&\quad (q_0 + q_1i + q_2j + q_3k)(h_{2,0} - h_{2,1}i - h_{2,2}j - h_{2,3}k)] \frac{1}{\|q\|^2}.
\end{aligned}$$

The expansion of the second term also involves a similar approach with quaternionic multiplication. Due to space limitation, we are not providing the detailed calculation for the second term. It is straightforward (but tedious!) to show that the real part of this second term is equal to $\|h_2\|^2 p_1$ and its i , j and k parts will not provide any information about p_1 and hence are irrelevant for its ML detection.

Therefore, we can claim that

$$\Re(\tilde{r}_2) = \Re(h_1(i\bar{p})\bar{h}_1 + h_2 \frac{\bar{q}\bar{p}i q}{\|q\|^2} \bar{h}_2)$$

contains sufficient information for ML detection of p_1 without any loss of information. Following the same approach, we can also show that $\Re(\tilde{r}_1)$, $\Re(\tilde{r}_3)$, and $\Re(\tilde{r}_4)$ are sufficient statistics for the ML detection of p_0 , p_2 and p_3 , respectively.

REFERENCES

- [1] G.J. FOSCHINI, *Layered Space-Time Architecture for Wireless Communication in a Fading Environment when using Multi-Element Antennas*, Bell Labs Technical Journal, 1:2(1996), pp. 41–59.
- [2] E. TELATAR, *Capacity of Multi-Antenna Gaussian Channels*, European Transactions on Telecommunications, 10:6(1999), pp. 585–596.
- [3] V. TAROKH, N. SESHADRI, AND A. R. CALDERBANK, *Space-Time Codes for High Data Rate Wireless Communications: Performance Criterion and Code Construction*, IEEE Transactions on Information Theory, 44:2(1998), pp. 744–765.
- [4] J. GUEY, M. P. FITZ, M. R. BELL, AND W. KUO, *Signal Design for Transmitter Diversity Wireless Communication Systems over Rayleigh Fading Channels*, IEEE Transactions on Communications, 47:4(1999), pp. 527–537.
- [5] V. TAROKH, H. JAFARKHANI, AND A. R. CALDERBANK, *Space-Time Block Codes from Orthogonal Designs*, IEEE Transactions on Information Theory, July 1999, pp. 1456–1467.

- [6] S.M. ALAMOUTI, *A Simple Transmit Diversity Technique for Wireless Communications*, IEEE Journal on Selected Areas in Communications, 16:8(1998), pp. 1451–1458.
- [7] B. HASSIBI AND B. HOCHWALD, *High-Rate Codes That Are Linear in Space and Time*, IEEE Transactions on Information Theory, July 2002, pp. 1804–1824.
- [8] H. EL-GAMAL AND A.R. HAMMONS, *A New Approach to Layered Space-Time Coding and Signal Processing*, IEEE Transactions Information Theory, 47:6(2001), pp. 2321–2334.
- [9] M.O. DAMEN, K. ABED-MERAIM, AND J.-C. BELFIORE, *Diagonal Algebraic Space-Time Block Codes*, IEEE Transactions on Information Theory, 48:3(2002), pp. 628–636.
- [10] M. O. DAMEN, A. CHKEIF, AND J.-C. BELFIORE, *Lattice Codes Decoder for Space-Time Codes*, IEEE Communication Letters, 4(2000), pp. 161–163.
- [11] M. O. DAMEN, H. EL-GAMAL, AND N. BEAULIEU, *On Optimal Linear Space-Time Constellations*, in: International Conference on Communications (ICC), May 2003.
- [12] S. N. DIGGAVI, N. AL-DHAHIR, A. STAMOULIS AND A. R. CALDERBANK, *Great Expectations: The Value of Spatial Diversity to Wireless Networks*, invited paper in Proceedings of the IEEE, pp. 219–270, Feb 2004.
- [13] H. JAFARKHANI, *A Quasi-Orthogonal Space-Time Block Code* *IEEE Communications Letters*, January 2001, 1-4.
- [14] A. NAGUIB, V. TAROKH, N. SESHADRI, AND A. R. CALDERBANK, *A Space-Time Coding Modem for High-Data-Rate Wireless Communications*, IEEE Journal on Selected Areas in Communications, October 1998, pp. 1459-1477.
- [15] N. SHARMA AND C.PAPADIAS, *Improved Quasi-Orthogonal Codes Through Constellation Rotation*, IEEE Transactions on Communications, March 2003, pp. 332-335.
- [16] B. L. VAN DER WAERDEN, *A History of Algebra: from Al-Khwarizmi to Emmy Noether*, Springer., New York, 1985.
- [17] A. ZHOU AND G.B. GIANNAKIS, *Space-Time Coding with Maximum Diversity Gains over Frequency-Selective Fading Channels*, IEEE Signal Processing Letters, 8:10(2001), pp. 269–272.
- [18] A. R. CALDERBANK, *A Four Dimensional Generalization of the 2x2 Alamouti Space-Time Code*, Presentation at the DIMACS Workshop on Algebraic Coding Theory and Information Theory. Rutgers University, New Jersey., December 2003.
- [19] L. HE AND H. GE, *A New Full-Rate Full-Diversity Orthogonal Space-Time Block Coding Scheme*, IEEE Communications Letters, December 2003, pp. 590-592.
- [20] V.ERCEG, K.V.S. HARI, M.S. SMITH, D.S. BAUM ET. AL., *Channel Models for Fixed Wireless Applications*, IEEE 802.16 Broadband Wireless Access Working Group, IEEE 802.16a-03/01, June 2003.
- [21] U. FINCKE AND M. POHST, *Improved Methods for Calculating Vectors of Short Length in a Lattice Including a Complexity Analysis*, Mathematics of Computation, 44(1985), pp. 463-471.
- [22] J.H.CONWAY AND D.H.SMITH, *Quaternions and Octonions*, Cambridge University Press, 2003.
- [23] M.ARTIN, *Algebra*, Prentice-Hall, 1991.
- [24] T. KAILATH AND A.H. SAYED, *Displacement Structure : Theory and Applications*, SIAM Review, 37(1995), pp. 297-386.

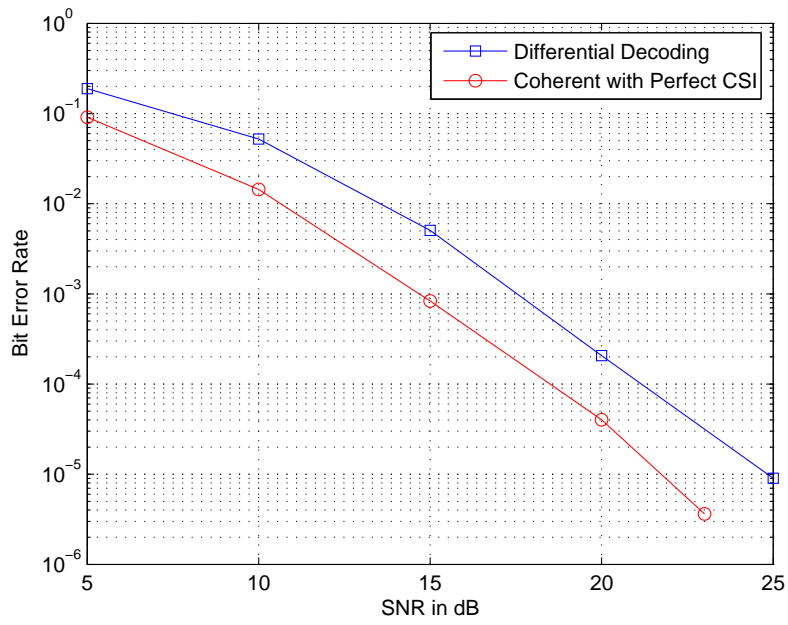


FIG. 5. Performance comparison between coherent and differential decoding in quasi-static fading.

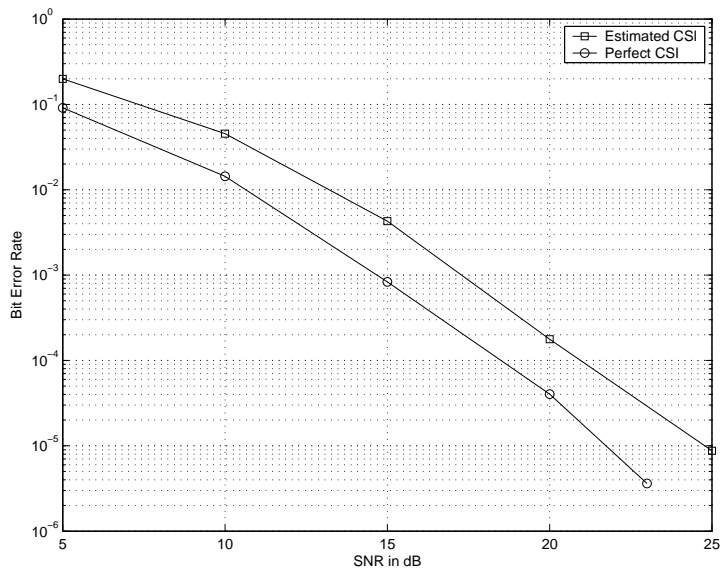


FIG. 6. Performance comparison between perfect CSI and estimated CSI in quasi-static fading.

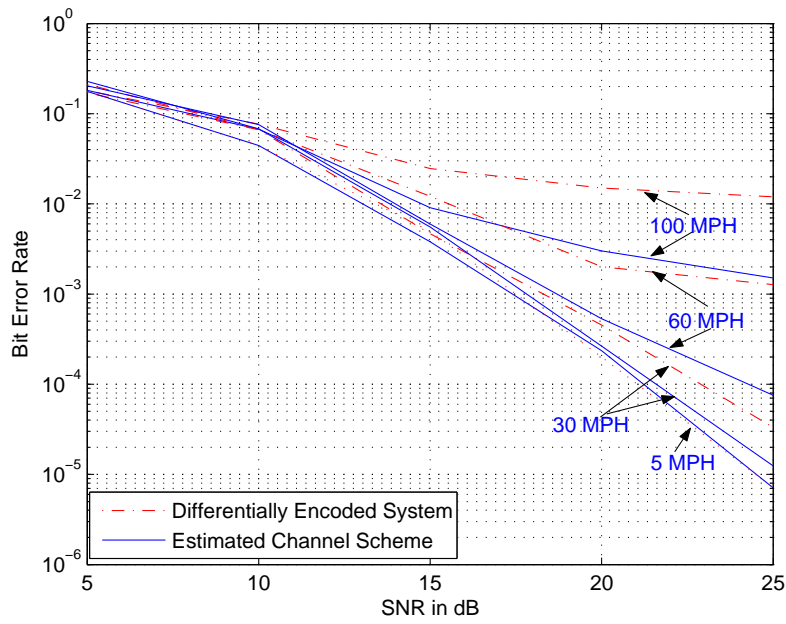


FIG. 7. Performance comparison between differential and pilot-based decoding schemes in time-varying channel.

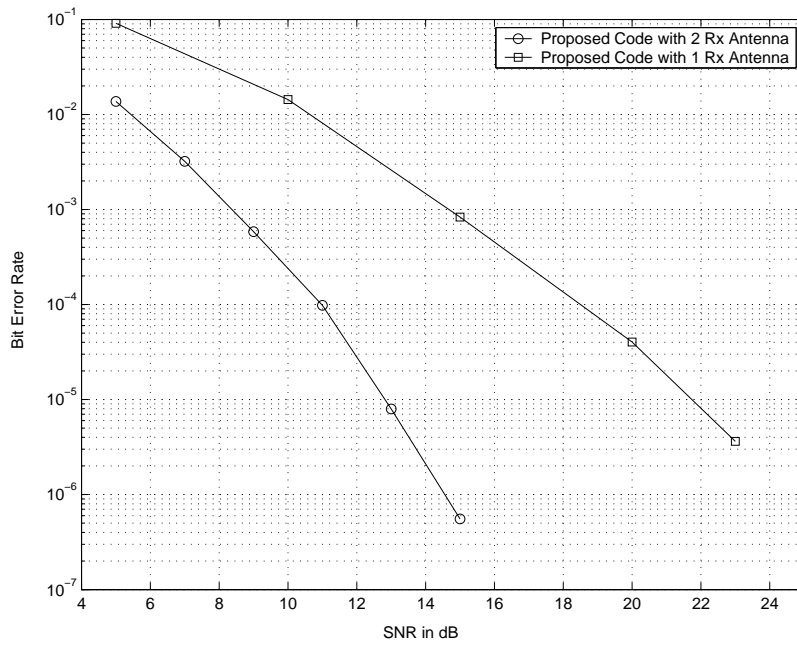


FIG. 8. Performance improvement by adding a second receive antenna.

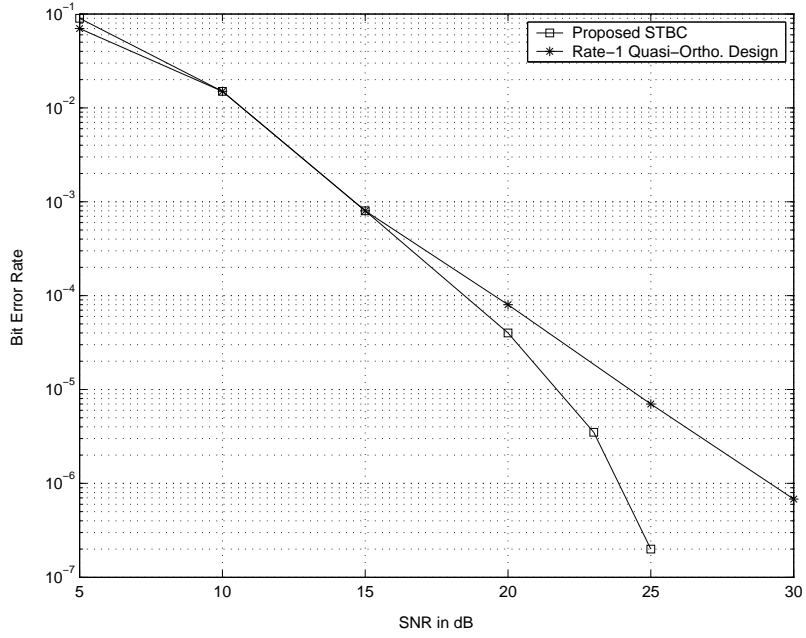


FIG. 9. Performance comparison between the proposed code and the rate-1 quasi-orthogonal design.

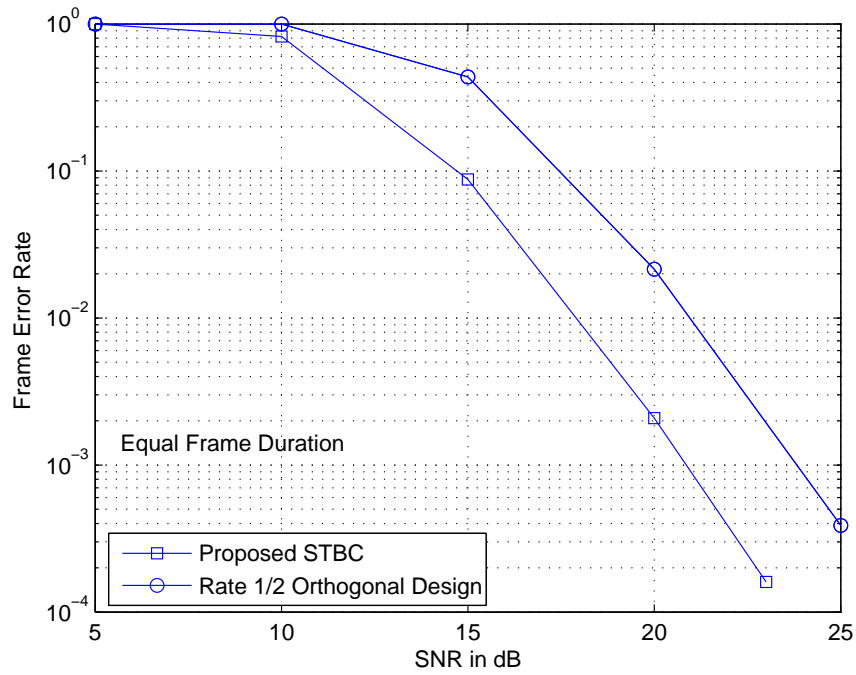


FIG. 10. Frame error rate comparison between proposed code and rate- $\frac{1}{2}$ orthogonal design at 2 bits PCU.

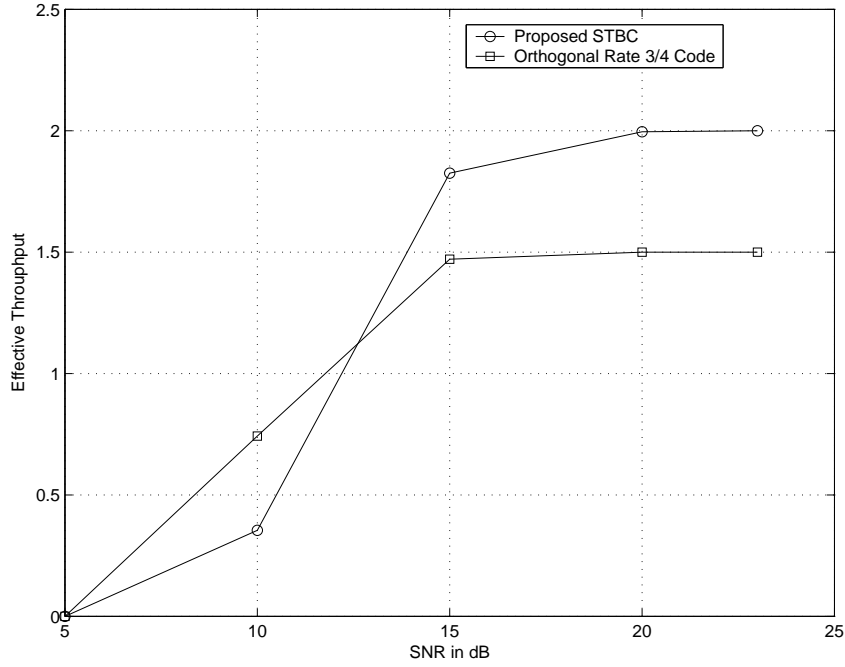


FIG. 11. Effective throughput comparison between proposed code and octonion code.

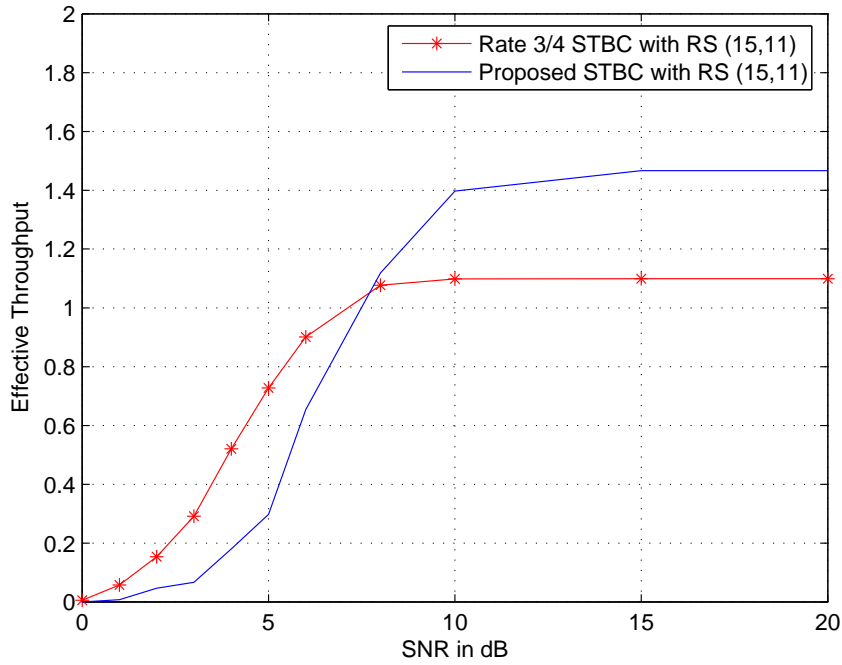


FIG. 12. Effective throughput comparison between proposed code and octonion code. Both are combined with an outer RS(15,11) code.

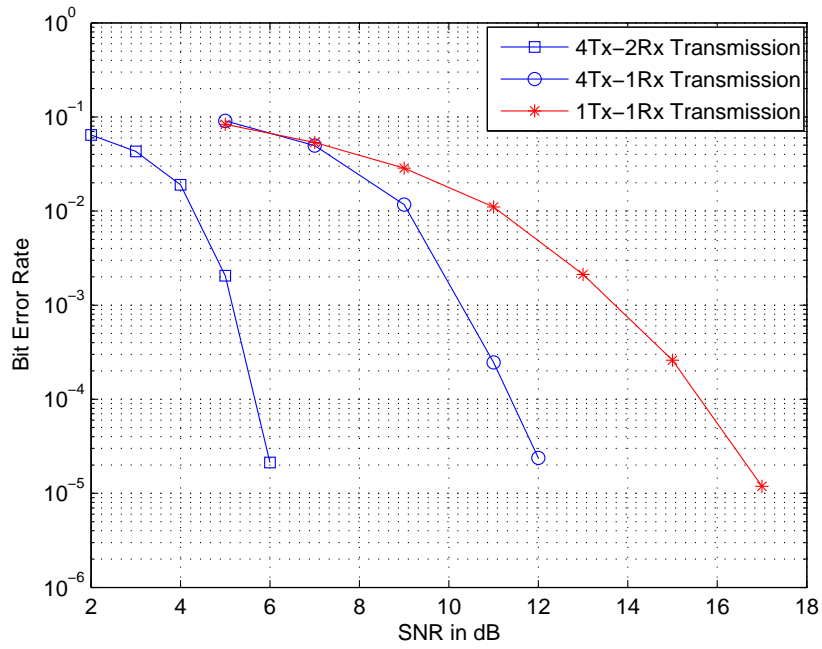


FIG. 13. Performance comparison between our proposed code (with 1 and 2 receive antennas) and SISO transmission. Both are combined with OFDM in an 802.16 scenario.